# 8

# Special Areas Detection and Recognition on Agricultural Fields Images

Valentin Ganchenko[1], Rauf Sadykhov[2], Alexander Doudkin[3], Albert Petrovsky[4], Tadeusz Pawlowski[5]

[1, 3, 4] *United Institute of Informatics National Academy of Science, Minsk, Belarus, ganchenko@lsi.bas-net.by*
[2] *Belarusian State University of Informatics and Radioelectronics, Minsk, Belarus, rsadykhov@bsuir.by*
[5] *Industrial Institute of Agricultural Engineering, Poznan, Poland, tadek@pimr.poznan.pl*

## 8.1 Introduction

Every year a need for information obtained using remote sensing data (RSD) is growing. RSD are used in problems of cartography and land cadastre [1], an agronomy and a precision agriculture [2-7], a forestry [8-11], a development of water systems [12], an environmental monitoring [13] etc. Constantly growing requirements for perfect data processing systems are increasing, because information is a key element in decision-making, and amount of information of different degrees of complexity increases. One of major problems arising in connection with creation of modern information systems is automation of processing of raw data presented as images.

One of the most important areas of image processing is a precision agriculture area. Efficient processing of raw data allows reducing material and other costs in problems associated with crop cultivation and forecasting, a monitoring of level of crops germination and many other applications. The solution of such problems involves using of geographic information systems (GIS), which combine necessary techniques for image processing. A number

of institutes and companies around the world deal with researches in this area, which include Research and Development Center "ScanEx" (http://www.scanex.ru/), the company ESRI (http://esri.com/), the company ERDAS, Inc. (http://erdas.com/). There are also a number of research centers that solve the problem of precision farming: Australian Centre for Precision Agriculture (http://www.usyd.edu.au/su/agric/acpa/pag.htm), Centre for Precision Farming (http://www.silsoe.cranfield.ac.uk/cpf/), Ohio State University Precision Agriculture (http://precisionag. osu.edu/) and others.

### 8.1.1 Thematic processing

Remote sensing methods allow effective detecting field areas that are infected by plant diseases. Detection and recognition of an infection on early stages of its development reduces costs of plant protective measures. There are two main approaches for detection of the infected areas: spectrometric and optical or visual [14-18]. The spectrometric approach allows detecting a number of infections on very early development stages. For example, a change of reflective features of potato plants in infrared area allows identifying phytophthora even before appearance of visual features [14, 17]. In spite of that fact a development of optical methods for infection detection takes place both for independent systems and for spectrometric ones what increases a quality of disease recognition of affected areas of agricultural fields. They should include the following ones:

- methods and algorithms for preprocessing and selection of features of the objects in agricultural fields images based on combining a spectral approach and a separation in space color coordinates;
- artificial neural network (ANN) models for fuzzy data clustering and classification methods.

The main stage of thematic image processing is image segmentation (groups of pixels), i.e. a separation of the image into homogeneous color or spectral characteristics areas by any criterion of homogeneity (similarity), and assigning them certain pre-defined classes [19-24].

Segmentation of image $f(x, y)$ by predicate $L_p$ is partition $S = \{S_1, S_2, \ldots, S_k\}$, which satisfies the following conditions:

a) $\bigcup_{i=1}^{k} S_i = X;$

b) $S_i \bigcap S_j = \varnothing$ for any $i \neq j;$

c) $L_p(S_i)$ is true for any $i$;

d) $L_p(S_i \cup S_j)$ takes false value for any $i \neq j$.

Note that $k$ resulted areas are often grouped into $m$ classes, where $2 \leq m \leq k$.

A majority known image segmentation methods, as well as methods of edge detection can be divided into two main groups: regional-oriented methods, which directly build $S_i$, and boundary-oriented ones, which determine boundaries of $S_i$ [25-29].

In methods of the first group a criterion for homogeneity of areas in $L_p$ is common features of image: an intensity or a chroma, a texture type, spectral properties f image, etc. This group includes methods for threshold separation, region expansion and area separation.

$$L_p(S_i) = |\| \nabla f(x,y) \| - \| \nabla f(x',y') \|| \leq T;$$
$$|\phi \nabla f(x,y) - \phi \nabla f(x',y')| \leq A;$$

where $\nabla$ is a gradient of function $f$; $\varphi$ is a direction of the gradient; $T$ and $A$ are thresholds.

Local analysis operators, such as Sobel, Roberts, Kirsch ones, are used for calculation of the gradient. In turn, convolution operators allow to directly select pixels that are, for example, may belong to straight line of a particular orientation and a width. A choice of a segmentation method depends on an ultimate goal of image processing, an image type and available computing powers. The most difficult task is to construct an algorithm for segmenting of agricultural fields images that are very noisy. As a rule a combination of some approaches provides a full solution of the problem of land cover recognition, especially using multi-temporal data.

The method of building areas in combination with using of deformable models is proposed to process digital aerial images [19]. This hybrid approach is called “a method of competition areas”. Deformable models are represented as a set of flexible curves that adapts to the contour vectorization of segmented area minimizing energy dynamically. The method includes the best features of the build-up method and the method of deformable models.

ANNs are actively used for processing of RSD of agricultural lands. For instance, neural network ARTMAP [30] based on adaptive resonance theory is used for mapping of vegetation according to spectral imaging and landscape data. An approximate fidelity of ARTMAP is about 80 %.

Modular ANNs are proposed to use for finding plants or areas of crops, contaminated by biological agents [31]. They reduce an influence of confounding factors and provide a classification of spectral curves of chemical components. An evaluation of a vegetation state, i.e. detection of

chemical components is based on processing of images of plant leaves. Modular ANNs can provide better results than traditional ANNs.

A mathematical morphology method is proposed for segmentation of gray-scale agricultural landscape images [20]. It is based on a watershed transformation and operations of a halftone pseudo skeleton building and is characterized by non-use of binarization operations that can significantly improve the quality of segmentation. The operation of the halftone pseudo skeleton building enables to carry out grayscale image segmentation with a significant reduction of effect of quantization and noise errors on the segmentation result. This feature helps to significantly reduce time of segmentation both in an analysis phase and in an areas association. For increasing of sensitivity it is proposed to use a number of morphological gradients computed for different structuring elements.

The system of accurately herbicide [32] uses a capturing and image processing based on the apparatus of fuzzy logic. Weeds are searched on images in shades of green color. The system automatically controls of herbicide application for effective removal of weeds, reducing cost of work and minimizing contamination of soil and water. Fuzzy logic membership functions are easily modified and allow to quickly creating control instructions for the system.

A technology of automatic rice field detection is proposed in [33]. The main feature of the technology consists in application of regional-oriented classification based on geographical data and a set of image region of interest during study period. It is studied normalized difference vegetation index over time for detecting rice fields.

Advanced Spaceborne Thermal Emission and Reflectance Radiometer (ASTER) [23] is used to locate and display of agricultural crops, soil and some types of a land cover. Four attributes of arable land are considered: planted culture, stages of yield growth, color and texture of soil. The user (operator of the system) carries out a classification using a minimum average distance.

Thus, there are a large number of algorithms that can be used for vegetation RSD processing. However, these algorithms are quite highly specialized and designed for specific tasks that can greatly reduce their results in application to the images of agricultural fields. Using of widespread algorithms is complicated by the complexity of the research object. Sometimes image processing is very difficult because of noises on images (foreign objects, sun glare on the leaves of plants etc.).

In this context a development of feature extraction algorithms are required. They can rely on expert data (for example, the expert can specify the different characteristics of the vegetation depending on the lighting). One should bear in mind that sometimes only gray-scale images are available. Hence, the algorithms providing additional features should be based only on this data.

Ultimately, it is needed a segmentation algorithm, which can be applied to both conventional spectral data and additional data (e.g., a texture).

### 8.1.2 Data processing system in task of vegetation monitoring

The basic concept of precision agriculture is the fact that a vegetation cover is not uniform within a single field. Up-to-date technologies are used to evaluate and detect these irregularities: global positioning systems (GPS, GLONASS), special sensors, aerial photographs and a satellite imagery, as well as special software system based on GIS. RSD are used for more accurately evaluation of a seeding density, calculation of application rates and crop protection, more accurate prediction of yield and a financial planning. Also, it must take into account local peculiarities of soil and climatic conditions. In some cases it may allow easier to adjudicate the reasons for deterioration of vegetation [7].

Sometimes precision agriculture is associated with desire to maximize profits applying fertilizers only on those portions of fields where fertilizers are needed. Following this, agricultural producers use technologies of variable or differential fertilization in those areas of the field, which are identified with help of GPS-receivers and where requirement for a certain rate of fertilizers is identified using yield maps. Therefore, a rate of application or spraying is less than an average in some areas of field, and a redistribution of fertilizers takes place in favor of areas where the rate should be higher, and thus, an application of the fertilizers are optimized.

Precision agriculture can be used to improve a state of fields in several directions:

- agronomical, taking into account real requirements of crop in fertilizers;
- technological, making better planning of agricultural operations;
- environmental, reducing negative impacts of an agricultural production on environment, for instance, a more accurate estimation of requirements of crop in nitrogen fertilizers leads to a restriction of using and spreading of nitrogen fertilizer or nitrate;

- economic, increasing efficiency of agriculture, including reducing costs for nitrogen fertilizers.

Other benefits for agriculture may be in an electronic recording and a storage of field work history and harvest, which may help in subsequent decision-making and in a preparation of special reports on production cycle.

### 8.1.3 Existing systems

There are a number of systems that are intended for commercial and research tasks for precision farming.

*MARS* (the Monitoring of Agriculture with Remote Sensing; the Joint Research Centre of the European Commission's monitoring of agricultural land, http://mars.jrc.it/) is intended to manage and control in agriculture: crop forecast, agricultural insurance, the interaction with environment. The system is based on an analysis of crop models using weather and GIS or GPS data, as well as RSD.

*VESPER* (Variogram Estimation and Spatial Prediction plus Error, the Australian Centre for precision farming, http://www.usyd.edu.au/agriculture/acpa/software/vesper.shtml) was designed for spatial prediction based on kriging, i.e. on optimal statistic interpolation [34]). It is intended to generate maps of a crop yield [35] based on digital relief models and evaluation of salinity of a upper layer of soil [36]. The system also allows performing kriging variograms of fields with an ability to manually adjust and fit them. Friendly interface allows to define boundaries of fields and to generate grid interpolation.

*Ag Leader Insight* (Ag Leader Technology Ltd, http://www.agleader.com/) is a complete package of tools for precision farming from planting to harvest (from development of a project on a desktop of computer to its implementation in the field). It uses one of the most popular in the world technology of grain yield monitoring and allows to create and view maps of a crop yield and a moisture content during harvest, get an instant information how a state of the field effects on the yield. SeedCommand provides complete control over operations of sowing, which varies depending on requirements of crops, using AutoSwath functions, which turn on and off sections of drills based on the map of the field and already planted areas. It reduces cross-seeding saving 3-12 % seeds and increases potential yield at same time.

*Systems of Topcon Positioning Systems* (The Topcon Positioning Systems Company, Inc., http://www.topconpa.com/) is a major producer of software and hardware control and monitoring systems for agriculture. Topcon equipment to optimize spraying, planting and fertilizing.

*AGRO-NET NG* (Engineering Center "GEOMIR", http://www.geomir.ru/) is GIS-based software and provides GIS database for each field, a review of cultivated crops to an agronomic analysis. The company GEOMIR also manufactures mobile GIS electronic data acquisition for agricultural needs and electronic circuits for statistical and thematic analysis of agricultural fields.

### 8.1.4 Research object

Agricultural field color images are an object of our research in the chapter (fig. 8.1). Rectangles show the same area of field received from 5 m height.

The purpose of the work consists in development of effective method of processing of vegetative covers color images received with help of high resolution digital shooting, and also its realization as a software for computer vision systems. In this case, a spatial resolution of image refers to size of square of original object, contained in one pixel. Lower value of this quantity equals higher spatial resolution of image. In this article, if side of square is less than 0.6 cm, a spatial resolution is considered as high, otherwise – as low.

Color, fractal and textural features of images are used as a basis for the areas detection method under consideration. These features have been successfully used in several investigations related to image processing [16, 18, 37-39]. A scientific idea of this investigation is a joint using named above features for detecting objects on agricultural field color images.

After special areas detection we need to solve the problem of a recognition for mapping of a disease. This can be done by recognizing the initial image or by recognizing the received special area. For the image recognition we used histogram analysis of RGB- and HSV-color features.

## 8.2 Special areas detection

### 8.2.1 Textures

Heterogeneity or frequency of small fragments is called a digital image texture. A characteristic feature of the texture is uniformity at a neighborhood

or a local level, i.e. at the level of groups of adjacent pixels with different brightnesses [40]. There are two main approaches to definition of textures:

- a texture is a set of repeated basic primitives (elements) with a different orientation in space;
- a texture is regarded as a kind of anarchistic and homogeneous aspect, not having pronounced edges.

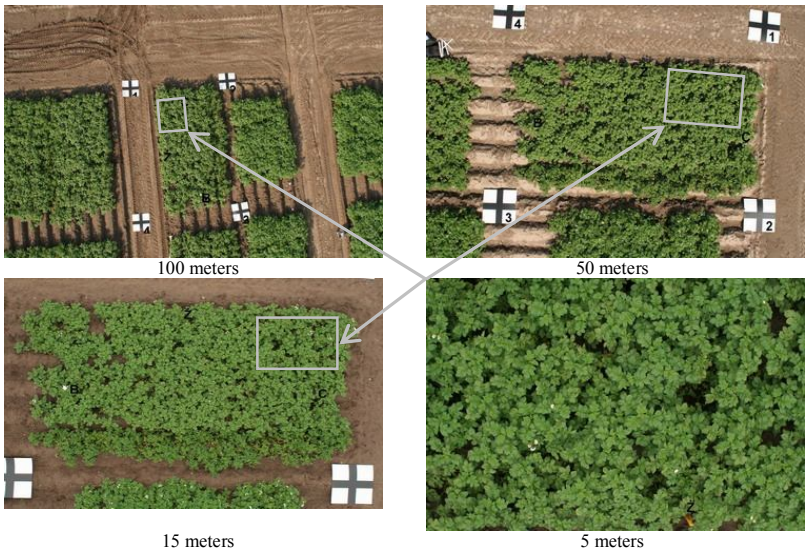


Fig. 8.1 Examples of initial aerial photographs

The texture are subdivided on fine-grained, coarse-grained, smooth, granulated and undulating in according with used base attributes and interactions between them. In view of interaction degree of the base elements the structures are subdivided on strong (interaction submits to some rule) and weak (interaction has casual character).

A texture is one of the major features used for identification of areas (objects) on the image. It represents two-level structure [40]:

- at the top level – a set of base elements connected by some spatial organization;
- on bottom – base elements representing casual aspect.

There are several methods to calculate textural characteristics [40]:

- methods based on measuring spatial frequency (high spatial frequencies are dominated on fine-grained textures, and low spatial frequencies – on coarse-grained textures);

- methods based on calculating a quantity of brightness jumps per unit of area (the quantity is small on coarse-grained texture ant it is increasing with a decrease in grain of the texture;

- methods using adjacency matrix of brightness (change in brightness distribution is much slower in coarse-grained textures than in fine ones with increasing a distance between evaluated points);

- methods describing textures by run lengths (lines of points with constant brightness is longer on coarse textures than on fine ones).Textural basic features are given below [41]:

$$ASM = \sum_{i=1}^{N_g} \sum_{j=1}^{N_g} \left( \frac{P(i,j)}{R} \right)^2; \quad (1)$$

$$Contrast = \sum_{n=0}^{N_g-1} n^2 \left( \sum_{\substack{i=1 \\ |i-j|=n}}^{N_g} \sum_{j=1}^{N_g} \left( \frac{P(i,j)}{R} \right) \right); \quad (2)$$

$$Entropy = -\sum_{i=1}^{N_g} \sum_{j=1}^{N_g} \left( \frac{P(i,j)}{R} \right) \log \left( \frac{P(i,j)}{R} \right). \quad (3)$$

An essence of the proposed method of textural features calculation consists in calculation of separate channel images signatures with their subsequent association with use of factors which values depend on vegetation type and condition. The example of textural features calculation is resulted in fig. 8.2, where the visualization of calculated values is resulted. Contrast approaches 1 at a small variation of initial data, and it decreases at greater variation. ASM approaches 1 at homogeneous initial data values. Entropy decreases to 0 at homogeneous color objects.

### 8.2.2 Fractals

In most cases natural objects on Earth's surface represent a fractal formation [42]. Whether an object is fractal, it is possible to determine qualitatively by considering it at different scales. There is no a natural length scale in fractal objects, and they look like equally for different image

enlargements [43, 44]. For example, tools for investigating electrical properties of natural objects are external electromagnetic fields of different frequencies. Each section of a surface has its conductivity at different frequencies. However, a fractality of objects means that a boundary of each conducting area is similar to a boundary of any other area at different frequencies in a statistical sense.

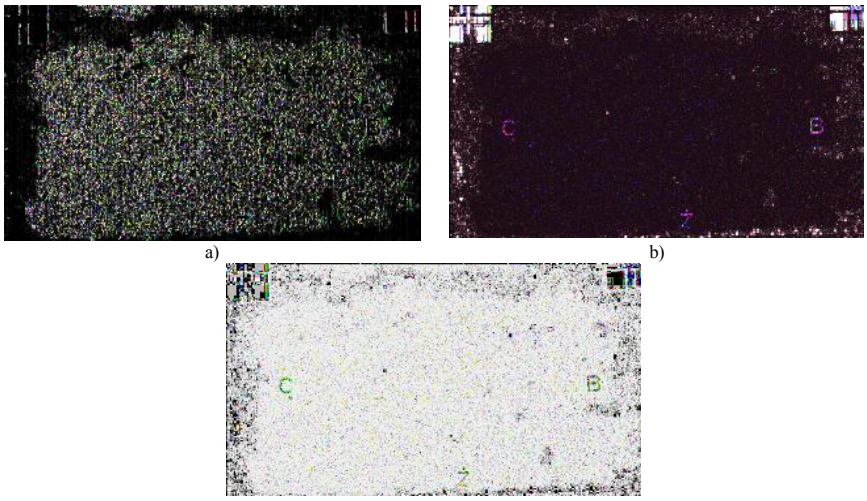

a) b) c)

Fig. 8.2 Result of textural features calculation for a field aerial photograph executed from height of 15 meters: a) Contrast; b) ASM; c) Entropy

Fractal theory can be used for segmentation of RSD, when fractal (fractional) dimension $D$ and fractal signature are used as a quantitative estimated parameter for segment descriptions [43].

Fractal signatures calculation is based on the fact that quantified intensity values of bidimentional signal are located between two functions named the top and bottom surfaces [42]. Top surface $U$ contains a set of points which values always exceed an intensity of the initial signal. Bottom surface $L$ has values of points which always are lower of the initial image (fig. 8.3).

The top and bottom surfaces are defined for at a zero point of initial as the following:

$$U(i,j,0) = L(i,j,0) = g(i,j); \tag{4}$$

where $g(i,j)$ is an initial image.

Generally we have:

$$U(i,j,\varepsilon+1)=\max\left\{U(i,j,\varepsilon)+1,\max_{k,m\in\eta}[U(k,m,\varepsilon)]\right\}; \tag{5}$$

$$L(i,j,\varepsilon-1)=\min\left\{U(i,j,\varepsilon)-1,\max_{k,m\in\eta}[L(k,m,\varepsilon)]\right\}; \tag{6}$$

$$\eta=\left\{(k,m)\,|\,d[(k,m),(i,j)]\le 1\right\}; \tag{7}$$

where $d$ is a distance function.

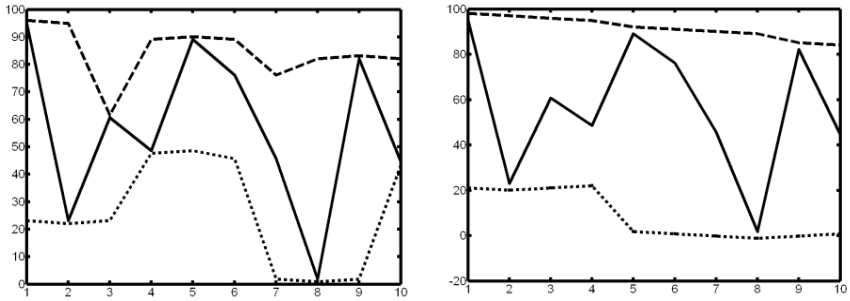

a) b)

Fig. 8.3 Constructing of top and lower surfaces:
a) ε = 1; b) ε = 3

The designed covering, formed by two specified functions, has thickness 2ε. For the bidimentional signal the area of a surface is the volume occupied with a covering, and divided on size 2ε. The "surface" area of intensity $A(\varepsilon)$ within the limits of window of observation ($R$) calculates by subtraction of bottom "surface" points from top with further summation on all window:

$$A(\varepsilon)=\frac{\sum_{i,j\in R}U(i,j,\varepsilon)-L(i,j,\varepsilon)}{2\varepsilon}=\frac{V(\varepsilon)}{2\varepsilon}. \tag{8}$$

A fractal dimension is determined by the slope of the *log* $A(\varepsilon)$ as function *log* ε. The example of the fractal signature is represented in fig. 8.4.

Fractal dimension $D(i,j)$ at point $(i,j)$ for all scales is defined as weighted sum of the local fractal dimension $F_\varepsilon(i,j)$:

$$D(i,j)=\frac{\sum_{\varepsilon}C_\varepsilon F_\varepsilon(i,j)}{\sum_{\varepsilon}C_\varepsilon}; \tag{9}$$

where

$$C_\varepsilon = \frac{\log \varepsilon - \log(\varepsilon - 1)}{\log 2}; \tag{10}$$

$$F_\varepsilon = \frac{\log A(i,j,\varepsilon) - \log A(i,j,\varepsilon - 1)}{\log \varepsilon - \log(\varepsilon - 1)}. \tag{11}$$

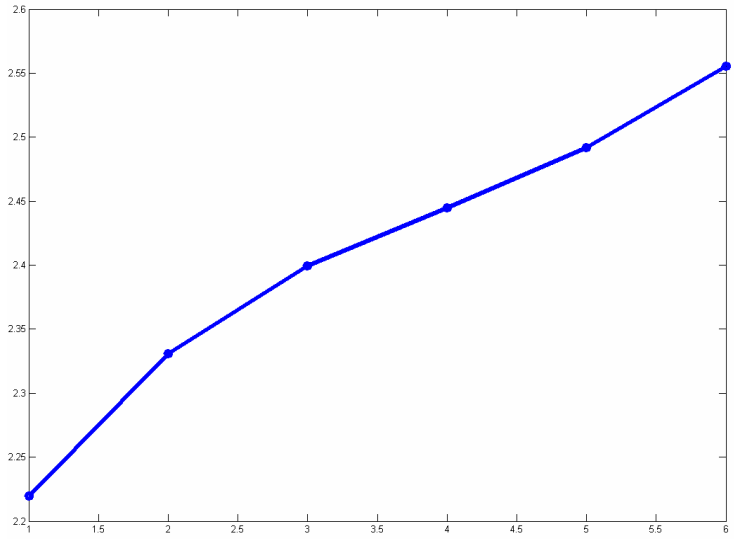

Fig. 8.4 Image part fractal signature

Size $F_\varepsilon(i,j)$ is calculated by division $A(i,j,\varepsilon)$ on $A(i,j,\varepsilon-1)$:

$$\frac{A(i,j,\varepsilon)}{A(i,j,\varepsilon-1)} = \frac{K\varepsilon^{(2-D)}}{K(\varepsilon-1)^{(2-D)}} = \left(\frac{\varepsilon}{\varepsilon-1}\right)^{(2-D)}; \tag{12}$$

after finding the logarithm, we obtain:

$$\frac{\log A(i,j,\varepsilon) - \log A(i,j,\varepsilon-1)}{\log \varepsilon - \log(\varepsilon-1)} = 2 - D = F_\varepsilon(i,j). \tag{13}$$

Having substitution of the values composed in (11) and (12) in expression (13) we obtain fractal dimensions evaluation:

$$D(i,j) = \frac{\log A(i,j,\varepsilon) - \log A(i,j,1)}{\log \varepsilon - \log 1}; \qquad (14)$$

Results of fractal signatures calculation are presented in fig. 8.5 (the visualization of the calculated values of fractal signatures is resulted). Fractal dimension $D$ approaches 2 at high irregularly and heterogeneity of initial data and reduces to 1 for homogeneous data.

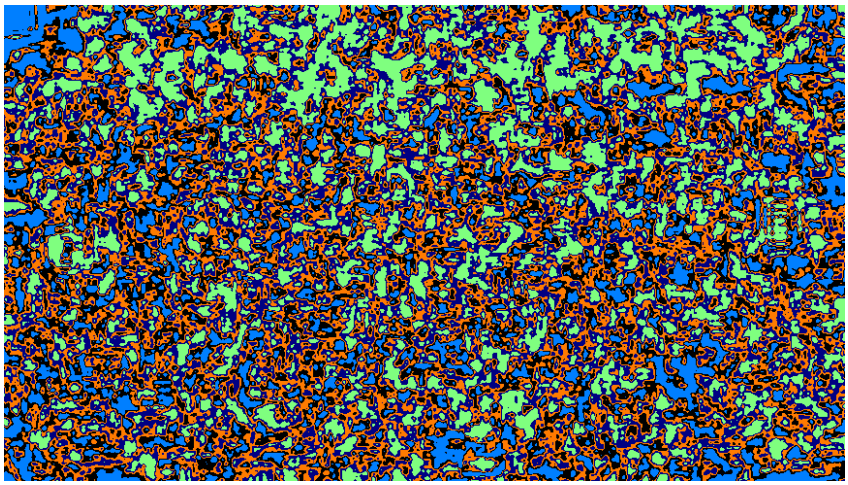

Fig. 8.5 Fractal signatures of various image areas

### 8.2.2 Processing algorithm based on joint segmentation

The essence of a segmentation algorithm is co-processing of source images and their fractal and textural features (i.e., an initial multispectral image is complemented by images of texture and fractal features).

Calculating of the fractal signature and textural features of the images is carried out for individual channels and their subsequent associations with using of coefficients whose values depend on a type and a condition of vegetation.

As a feature space, on which a decision is made, a weighted matrix of color features of the initial image, as well as the textural and the fractal features computed for each color channel of the initial image are used.

Color ranges of corresponding healthy and sick parts of fields obtained by expert are used as a color features.

The algorithm is intended for segmentation of bidimentional data representing matrices of various features of the initial image such as color channels, textural and fractal characteristics. Thus, the segmentation algorithm is carried out in *N*-dimensional space of attributes (where *N* is a quantity of the used characteristics) where each dimension can be considered with a certain weight coefficient.

Thus, the algorithm consists of the following steps (Fig. 8.6).

**Step 1.** Processing of initial images for receiving of additional information of channels representing matrices of textural and fractal characteristics of each initial image color channel separately;

**Step 2.** Joint segmentation of the received matrices of textural and fractal characteristics and initial images color channels (it is carried out by K-means or ISOMAD algorithm);

**Step 3.** Special areas maps building on basis of results of the joint segmentation.

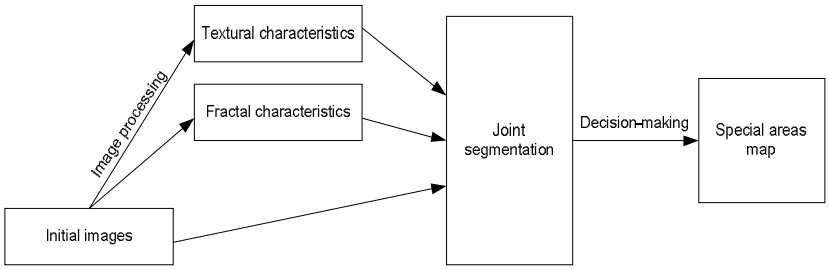


Fig. 8.6 Processing algorithm scheme

An example of execution of the processing algorithm based on joint segmentation applied to the image shown in Fig. 8.7. Obtained segmentation result allows in an automatic mode to detect areas on which there is a disease development. A knowledge of an allocation of such areas allows determining requirement of those or other agricultural fields areas for fertilizers and other chemicals. It allows making agricultural works more effective and less expensive.

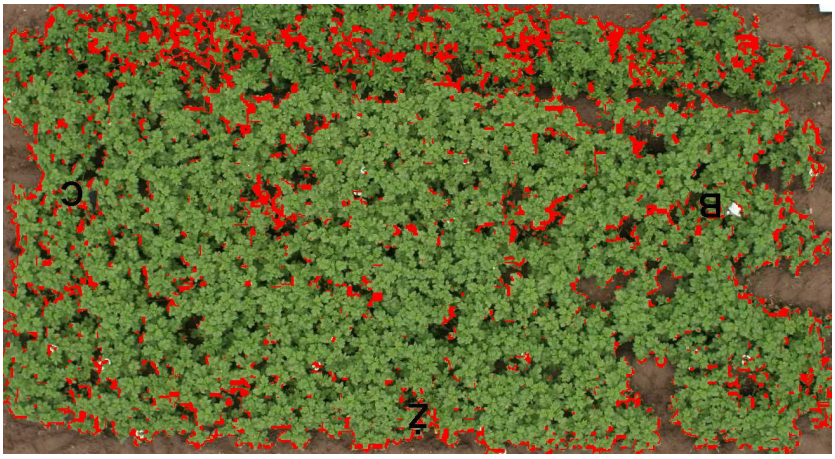

Fig. 8.7 Joint segmentation result example

## 8.3 Image recognition

### 8.3.1 RGB

Analysis of color features of various objects types in images showed that they differ slightly within the same type, and they are independent both of a height from which the images are taken, and of time of shooting. These color differences for each color channel (*R*, *G*, *B*) are offered to use for monitoring of agricultural fields diseases.

It should be noted that a histogram with a maximum global peak depends on size and color of images, on which it is constructed – for small images a size of individual elements of brightness can be set to zero, and the number of such elements may also decreases, that also leads to histogram distortions. To reduce an influence of these factors a histogram of brightness ranges is proposed to use, i.e. the histogram based on a set of elements of brightness in each range. Such histogram is referred to as a reduced one (or a histogram with the reduced number of readings along axis *X*). To ensure interoperability between the histograms of various sizes of the images we use a normalization procedure, after which the –the data take the values in range [0, 1].

Figure 8.9 illustrates an influence of quantity of the ranges on the reduced and normalized histograms for the images of different classes of objects

shown in Figure 8.8, where solid, dashed and dotted lines indicate the histograms of red, green and blue channels respectively. Histogram distortions are seen in Figures 8.9d-8.9f – a smoothness decrease and an appearance of a large number of gaps, i.e. regions with zero values in the histogram. A loss of data also can be seen by comparing Figures 8.9b and 8.9c or Figures 8.9e and 8.9f (a detail is missing if the number of segments is reduced from 64 to 16. In this case a difference of color features of objects of various types may be insufficient for classification (Figure 8.9c, 8.9f, 8.9i). To minimize a data loss specified by variability the number of the ranges should be chosen so that the reduced histogram gets smoother than the original one, but contains enough data about the variability. The partition to 64 segments on *X* axis was selected during the experiments.

a) b) c)

Figure 8.8 Image of diseased plants areas with size 97x66 pixels (8.8a) and 20x32 pixels (8.8b), area of healthy plants with size of 62x50 pixels (8.8c)

A normalized histogram for one color channel of an image of size *M*x*N* pixels is formed by the following algorithm:

**Step 1**. Calculating histogram (*hist*) for the selected image areas. The histogram is an array of numbers of range [0,255], each number represents an amount of elements of specified brightness on a halftone image.

**Step 2**. Calculating reduced histogram (*hist*) with 256 points to 64 values – amount calculated for each segment containing four values of original histogram:

$$res(i) = \sum_{k=(i-1)*4+1}^{i*4} hist(k), \text{ for } i = 1, \ldots, 64, \tag{15}$$

where *res* – an histogram array with reduced number of elements.

**Step 3**. Calculating the maximum value of histogram (*res*):

$$mx = \max(res(i)), \text{ for } i = 1, \ldots, 64, \tag{16}$$

**Step 4**. Normalization of histogram (*res*) to the range [0, 1] by dividing values res of the histogram array on *mx*:

$$res(i) = res(i) / mx, \text{ for } i = 1, \ldots, 64, \tag{17}$$

This algorithm is used for each color channel of the original image. As a result, three normalized reduced histograms are obtained, that together make up an array of 192 values, which is used for classification.

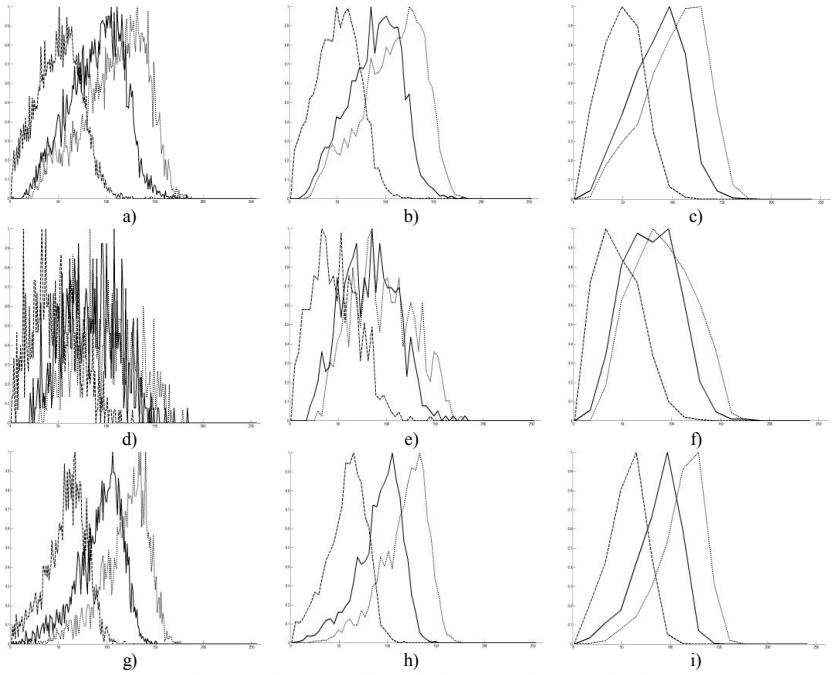


Figure 8.9 Histograms: the original (8.9a, 8.9d, 8.9g), reduced to 64 segments (8.9b, 8.9e, 8.9h), up to 16 segments (8.9c, 8.9f, 8.9i) for objects 8.9a, 8.9b, 8.9c respectively

### 8.3.2 HSV

Color space HSV (Hue, Saturation, Value) can be used in addition to color space RGB. To go from RGB to HSV should The following transformations are performed to obtain HSV representation of given RGB image.

1. Converting RGB channels with range [0, 255] to range [0, 1] by dividing color values of pixels of the image by 255.

2. Calculating HSV color values by the following formulas:

$$H = \begin{cases} 0, \text{ если } \max(R,G,B) = \min(R,G,B); \\ 60 \times \dfrac{G-B}{\max(R,G,B) - \min(R,G,B)} + 0, \text{ если } \max(R,G,B) = R, G \geq B; \\ 60 \times \dfrac{G-B}{\max(R,G,B) - \min(R,G,B)} + 360, \text{ если } \max(R,G,B) = R, G < B; \\ 60 \times \dfrac{B-R}{\max(R,G,B) - \min(R,G,B)} + 120, \text{ если } \max(R,G,B) = G; \\ 60 \times \dfrac{R-G}{\max(R,G,B) - \min(R,G,B)} + 240, \text{ если } \max(R,G,B) = B; \end{cases} \quad (18)$$

$$S = \begin{cases} 0, \text{ если } \max(R,G,B) = 0; \\ \text{иначе } 1 - \dfrac{\min(R,G,B)}{\max(R,G,B)}; \end{cases} \quad (19)$$

$$V = \max(R, G, B). \quad (20)$$

where $H$ possesses the values in range [0, 360), and $S$, $V$, $R$, $G$, $B$ – in range [0, 1].

3. Transforming values $H$, $S$ and $V$ to range [0, 255]:

$$\begin{aligned} H &= H / 360 \text{ x } 255; \\ S &= S \text{ x } 255; \\ V &= V \text{ x } 255. \end{aligned} \quad (21)$$

Further, the proposed image processing algorithms are applied to HSV data. RGB-data – construct normalized reduced histograms. Figure 8.10 shows the normalized histograms for reduced HSV color space, where solid,, dashed and dotted lines shows the values of channels Hue, Saturation and Value respectively.

### 8.3.3 Perceptron as classifier

The task of object classification on images is partially solved by using texture feature Contrast of quantity measure s measure of local variations on the images. Depending on degree of image variability textural feature Contrast takes higher values for images having high divergent objects and lower values – in case of low divergent objects. Analysis of texture feature Contrast showed that the soil plots are low divergent and areas of vegetation – high divergent [45]. Thus, Contrast can be used to separate image plots of soil. This will reduce the amount of computation that may be important in processing large amounts of data. In contrast to soil, leaves of vegetation are equally low divergent on images of high spatial resolution. A high variability

is preserved only at edges of leaves, which does not correctly separate classes of "soil" and "vegetation". To use the texture feature Contrast for mapping image areas containing soil, some transformations should be performed. It is proposed not to use arrays of features of channel images but halftone images, those visualize the arrays.This allows expert to monitor and adjust process as well as widespread use of image processing algorithms for conversion.

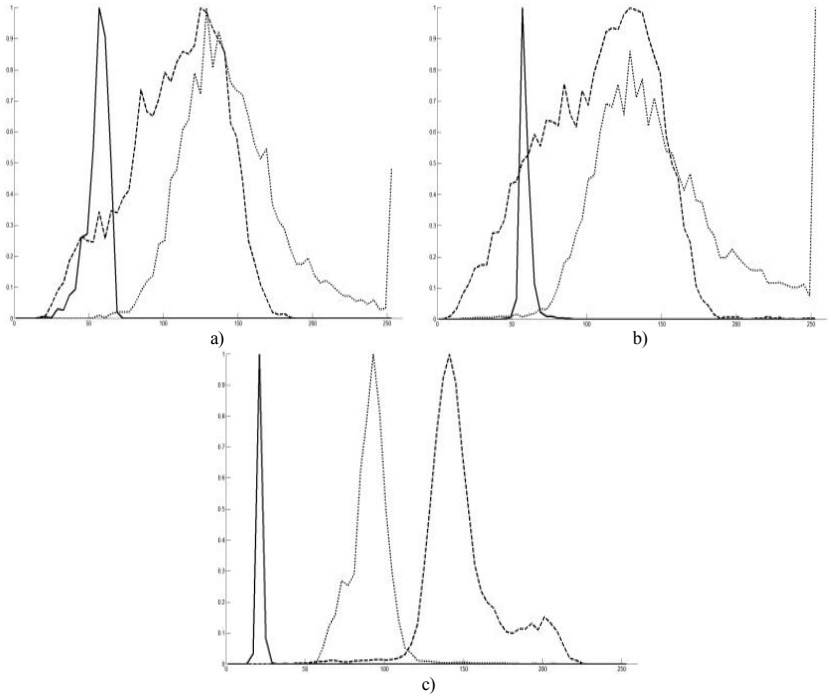


Fig. 8.10 Normalized reduced histogram constructed for the HSV-representation: a) “diseased plants”; b) ”healthy plants”; c) ”soil”

To classify image areas a multilayer perceptron [46] is proposed to use with $N \times L$ inputs (where $N$ – a number of segments of the reduced histogram, $L$ – a number of channels), one hidden layer, containing $32 \times 3$ neurons (the number of the neurons is chosen experimentally), and an output layer containing three neurons corresponding to object types of the images. All neurons have a logistic activation function in a sigmoid form.

The back-propagation algorithm is used to adjust weights of the perceptron. In this case, the input of the perceptron fed normalized

histograms obtained from images of objects selected by an operator. A data sample for learning algorithm is formed by scanning the original image through a "running-window" size *K*x*K*.

Training of perceptron performed on low resolution images of one type objects related to one of indicated classes selected by an expert (100 images for each class). Peculiarities of lighting and spatial resolution were not considered because of the training set contains images with different lighting conditions and with different spatial resolution.

Classification of images of high spatial resolution is carried by the following algorithm (Alg 1a):

**Step 1**.Select next area of a source image by a "running-window".

**Step 2**. Build an normalized reduced histogram for chosen area for each color channel.

**Step 3**. Perform pixel classification by the multilayer perceptron.

**Step 4**. Assign a class obtained in step 3 to the point in center of "running-window".

**Step 5**. Form a map of morbidity rate from the obtained values of classes of objects

Classification of images of low spatial resolution is carried by the following algorithm (Alg 1b):

**Step 1**. Construct a mask of vegetation using features Contrast.

**Step 2**. If the image is processed completely, then go to step 7, otherwise choose an element from the source image by "running-window".

**Step 3**. If the mask of vegetation in center of the "running window" is not zero, then go to step 4, otherwise assign a point in center of the "running window" class "soil" and go to step 2.

**Step 4**. Build for selected "running-window" element normalized reduced histogram for each color channel.

**Step 5**. Perform pixel classification by the multilayer perceptron.

**Step 6**. Assign a point in center of "running-window" class derived in step 5.

**Step 7**. Form a map of morbidity rate from the obtained values of classes of objects.

Selection of image area and corresponding vegetation mask area carried out by means of "running-windows".

Figure 8.11 shows results of testing the algorithm. Selection of image areas was carried out by running-window of size $K \times K$ pixels without a mask (Figure 8.11b, 8.11d) and with the mask (8.11c, 8.11e) (in the experiments value $K = 10$ is used). The mask is formed from vegetation maps obtained

using feature Contrast. In Figures 8.11b, 8.11c, 8.11d and 8.11e non classified boundary are black, soil areas are dark gray, areas with healthy plants are light gray and areas of diseased plants are white.

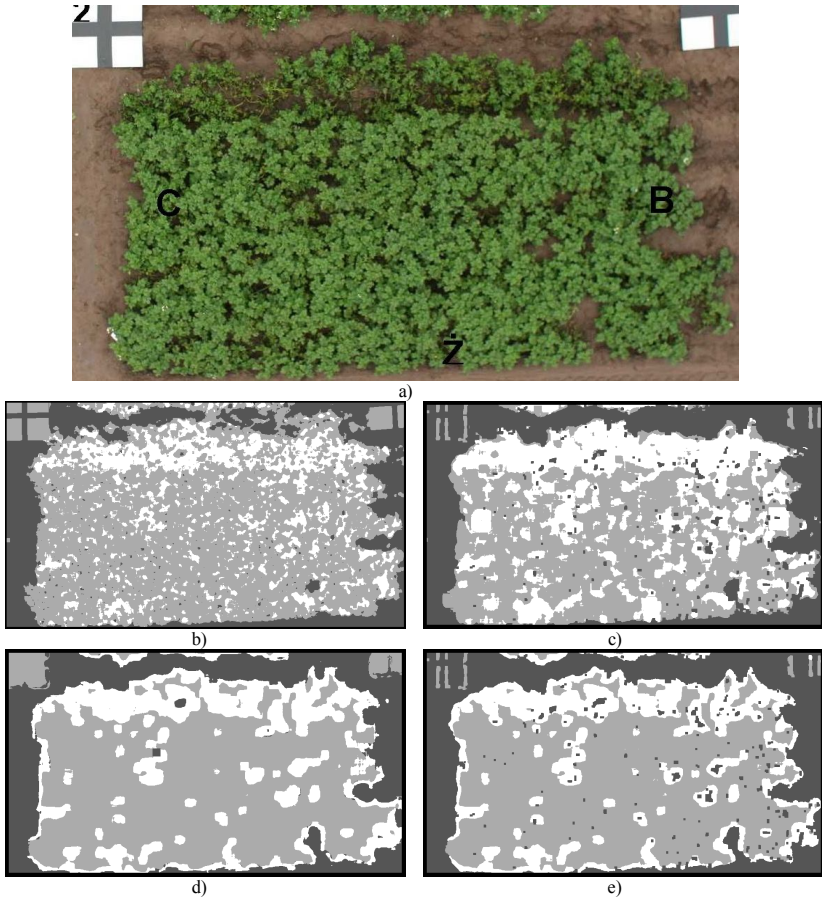


a)



b) c) d) e)

Fig. 8.11 Example map of disease for $K = 10$,used RGB-and HSV-submission: a) original image of a field; b) map of disease, "running-windows" without the mask (RGB); c) map of disease, "running-windows" with the mask (RGB); d) map of disease, "running-windows" without the mask (HSV); e) map of disease, "running-windows" with the mask (HSV)

The results of the experiments show that the algorithms applied to RGB images are more sensitive to details that create more shallow areas classifying as "diseased plants". At the same time the details are not lost by using HSV image representation. This distinction allows obtaining maps of

incidence varying detail, and thus more flexibility is appeared to recognition on the extent of diseased plants.

## 8.4 Recognition accuracy improving

### 8.4.1 Cluster recognition

A significant disadvantage of the algorithm described above is not sufficiently high recognition accuracy, due to the heterogeneity of vegetation, patches of sunlight on leaves, extraneous objects, etc. Masks of object classes can be used to increase recognition accuracy. Each mask is a binary image where areas of a particular class are marked by white color.

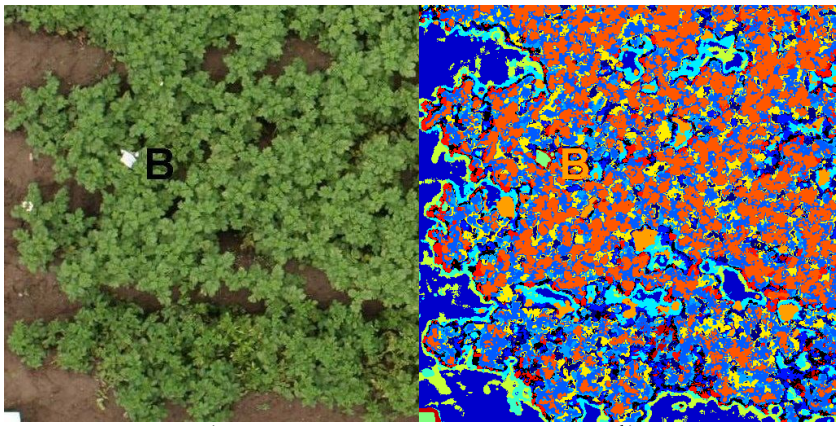

a) b)

Figure 8.12 Initial image (a) and result of clustering using GGC-algorithm for 15 clusters (b)

Recognition of clusters obtained as a result the joint segmentation can be used for construction of the masks of the classes. The algorithm includes next steps (Alg 2):

**Step 1.** Conduct a clustering of the initial image using joint segmentation algorithm, using color, texture and fractal features of images (see Figure 8.12).

**Step 2.** Obtain a binary mask for each of the obtained clusters, where 0 corresponds to areas not belonging to this cluster, and 1 – in another case (see Figure 8.13).

**Step 3.** Construct a reduced normalized histogram for each cluster in accordance with the obtained binary masks (for both RGB and HSV data representation).

**Step 4**. Recognize each of the resulting reduced normalized histograms using the trained neural network.

**Step 5**. Compose of the cluster binary masks and the images colored in accordance with the recognition results (see Figure 8.14).

Thus, the image is formed as a result of the algorithm. The classes of area objects on the image of agricultural fields («soil», «healthy plants» and «diseased plants») are marked with different colors. An example of recognition results is presented in Figure 8.13, where the dark gray areas denote corresponding class «soil», light gray ones – class «healthy plants» and white ones – class «diseased plants».

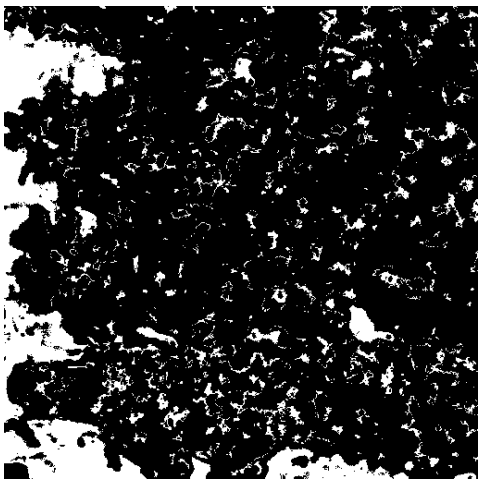

Figure 8.13 The binary mask of one of the clusters obtained by segmenting of the original image 8.12a

### 8.4.2 Comparison of recognition results

An evaluation of recognition accuracy of the proposed algorithms is presented in Table 8.1 (an error is calculated as the average error of recognition received for several images).

It is evident from Table 8.1 that using of the mask of «diseased plants» class, received recognition of clusters, allows improving recognition accuracy

significantly for initial agricultural fields images.

Thus, the algorithm for clusters recognition (Alg 2) can be used to increasing recognition accuracy by forming a class binary mask. The algorithm of image areas recognition (Alg 1) is basic of clusters recognition procedure. At the same time it can be used without masking (e.g., for mapping of diseases) and with masking (for statistics).

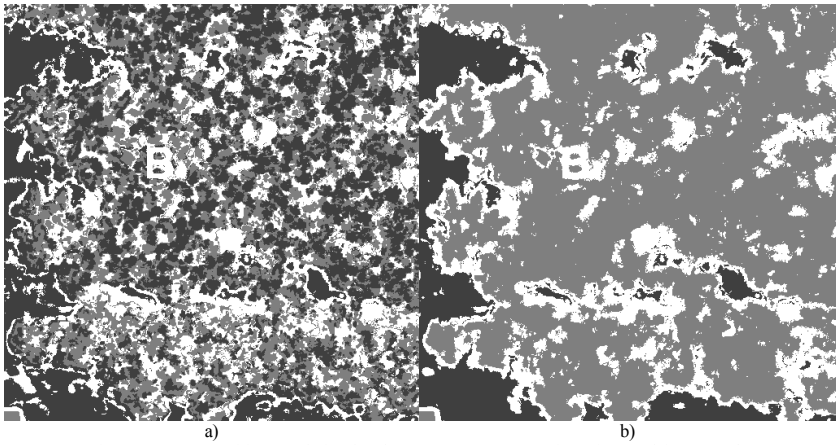

a) b)

Figure 8.14 Recognition result for the cluster RGB-representation of (a) and for HSV (b)

Table 8.1 Recognition errors

| **Algorithm** | **With mask** | | **Without mask** | |
|---|---|---|---|---|
| | RGB | HSV | RGB | HSV |
| By recognition of initial image areas selected by "running window" ($K$=10) | 4.835 | 4.957 | 20.028 | 16.888 |
| By recognition of initial image areas selected by "running window" ($K$=20) | 5.541 | 4.835 | 23.155 | 21.65 |
| By recognition of initial image areas selected by "running window" ($K$=30) | 5.591 | 6.132 | 24.15 | 24.996 |

## 8.5 Practical applications

On the basis of the developed algorithm the hardware-software complex for mineral fertilizers and other chemicals application on agricultural fields

has been proposed (Fig. 8.15). The technique based on the complex is the following.

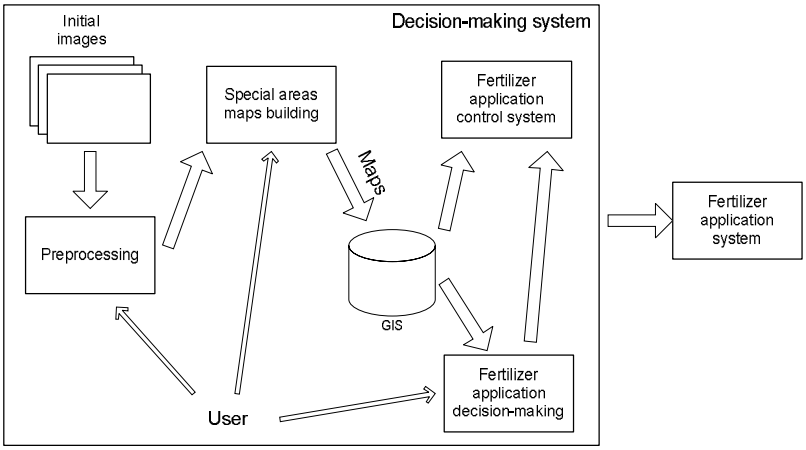


Fig. 8.15 Scheme of the hardware-software complex for mineral fertilizers and other chemicals application on agricultural fields

1. Special areas maps (for example, sites with developing disease of plants) are calculated with use of the proposed algorithms;

2. The-built maps receive a geographical binding and they are kept in DB GIS for further use;

3. The obtained maps are used at decision-making on necessity of application of this or that amount of fertilizers on that or other site of farmland;

4. Chemicals application control system on the basis of available maps and real-time data supervises amount of chemicals brought in soil and directs a corresponding command to chemicals application system.

The following real-time data can be used:

- data of a global navigating satellite system. In this case the control system, determining with help of the navigating system, on what site of a field a chemicals application is necessary, calculate the amount of chemicals, proceeding the corresponding special areas map;
- data of global navigating satellite system. In this case the control system, determining with help of navigating system, on what site of a field is calculates necessary amount of chemicals, proceeding from the special areas map;

- data from color camera in visual range. In this case the control system can correct in real time the given special areas maps, thus, making of more exact decisions that increases efficiency of chemicals application.

Generalized structural schema of software is shown in figure 8.16.

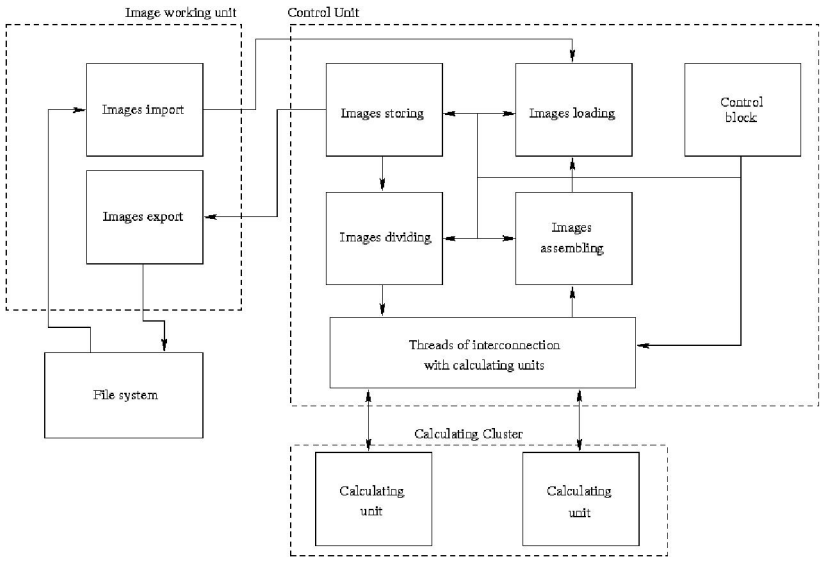


Fig. 8.16 Generalized structural schema of program system

The software system contains three main units:

1. Image processing unit. Tools of the unit allow storing, processing and keeping up integrity of geographical data, represented as raster images. The unit implements the following functions:

1.1. Image import. It is destined for translation of raster images stored at the file system to system internal format.

1.2. Image export. It is destined for translation of system internal format to raster images.

2. Control unit. This unit is destined for realizing of coordination calculating process, dividing of source image to parts, assembling result of image processing from parts. Unit contains three elements.

2.1. Calculations control. This unit is destined for realizing of control at stages of image processing.

2.2. Loading of data/Storing of result.

2.3. Dividing/Assembling of image

3. Calculating cluster. At this system unit parallel processing of source image parts is realized.

3.1. Processing unit. This unit realizes directly data processing.

Image processing is realized in the following way:

Source image is divided to parts. Each part contains some section of original multispectral image. Example of simple dividing is shown in figure 8.17. Some image processing algorithms requires taking into consideration environment of image element. In this case image element environment should be added to this element, as it is shown in fig. 8.18.

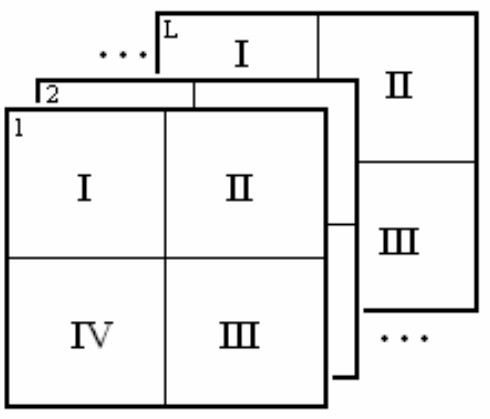


Fig. 8.17 Example of simple image dividing

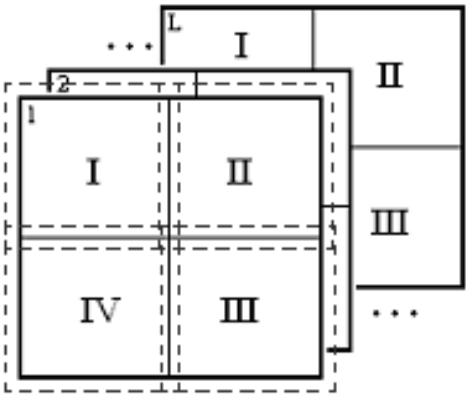


Fig. 8.18 Example of dividing with taking into consideration environment of image element

After dividing image to parts processing stage follows. At this stage realizes parallel multispectral image processing by parts.

Processing technology MPI (Message Passing Interface), which is explained in detail in [47], was selected as basis of parallel. This technology was selected because it allows simple organizing interaction of calculating units and them synchronization.

TCP connection, which allows transmit required data without losing, is used for data exchange between calculating and control units. At the same time interaction must be equal for each connection with corresponding calculating unit. Also this interaction must happen parallel for decreasing of performance losses when realizing interaction. It can be realized by allocation of individual thread for service each data exchange connection between corresponding calculating and control units. Multithreading using in GNU/Linux environment is explained in detail in [48].

Schema of system working is shown in figure 8.19. Tests of system of processing of images were made on a supercomputer «SKIF K-1000» [49, 50]. At carrying out of experiments it was involved from 1 up to 64 computing nodes for color images in the size 2000×2000 and 1000×1000 pixels. Dependence of an operating time of system on a number of the involved computing nodes is resulted on the graphs shown in figure 8.20.

## 8.6 Conclusions

The analyses of a problem of special areas detection and recognition on agricultural fields images reveals a lack of methods and algorithms for selection and classification of areal objects in multi-temporal images of agricultural fields with different spatial resolution. To solve this problem, analysis of subject area is carried out. As result it was found that direct application of any of existing methods do not provide full solution of the problem of detection and land cover classification of agricultural fields using multi-temporal data.

Algorithm for computing texture and fractal features is one of research results. They can be used as additional informative features for segmentation of images, which are contain foreign objects.

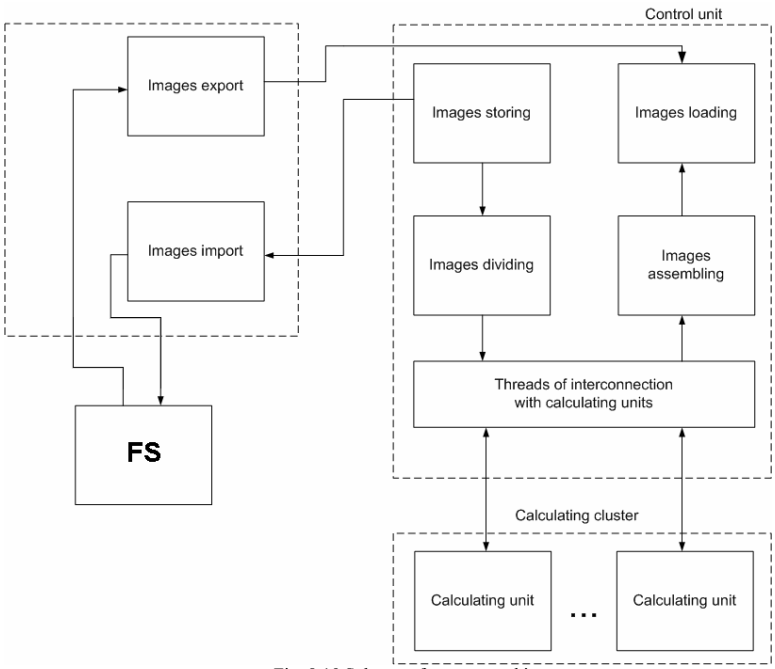


Fig. 8.19 Schema of system working

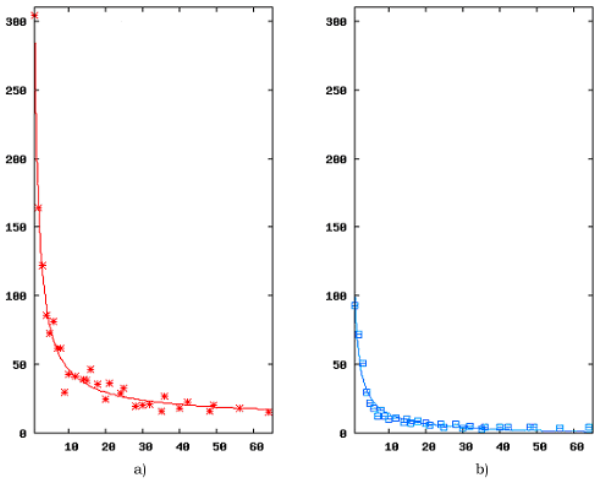


Fig. 8.20 Graphs of dependence of an operating time of system from a number of the involved nodes for color images in the size 2000×2000 (a) and 1000×1000 (b) pixels

The result of this work is algorithm of joint segmentation of agricultural field images, using color characteristics and evaluations of local variability of detected areas of vegetation affected by disease. By using additional information signs result in a lesser degree depends on light conditions and presence of foreign objects in image than when using only color features.

To solve the problem of agricultural field images classification, analysis of crop plants images color features is carried out. The analysis of aerial photographs of agricultural fields is based on an analysis of photographs of individual plants. As a result, it has been determined color characteristics of various diseases, as well as a number of features that are present in images, which can affect quality of classification.

The algorithms of constructing of reduced normalized histograms (using RGB and HSV-view of images), and classification algorithms based on using of color features represented in form of reduced normalized histograms, and taking into account spatial resolution of source images are proposed.

Thus, as a result of the work a number of algorithms allow to solve the problem of monitoring of agricultural plants state on basis of classification of color characteristics and using of texture and fractal features to improve classification accuracy are received.

The scientific importance of the obtained results consists in capability of creation of new highly effective methods and high-efficiency algorithms of no anthropogenic origin objects images processing and fractal nature objects allocation.

The practical importance consists of application of the developed methods and algorithms for natural origin objects allocation that allow increasing essentially accuracy and reliability of functioning of computer vision systems, monitoring and decision-making.

Possible area of application is remote sensing of the Earth (in forestry, geology, agriculture).

## 8.7 References

1. Bonnefon, R. Geographic information system updating using remote sensing images / R. Bonnefon, P. Dherete, J. Desachy // Pattern Recognition Letters. – 2002. – Vol. 23. – P. 1073-1083.

2. Multi-sensor NDVI data continuity: Uncertainties and implications for vegetation monitoring applications / W.J.D. vanLeeuwen [et al.] // Remote Sensing of Environment. – 2006. – Vol. 3. – P. 67-81.

3. Sofou. A. Soil image segmentation and texture analysis: a computer vision approach / A. Sofou. G. Evangelopoulos, P. Maragos // IEEE Geoscience and Remote Sensing Letters. – 2005. – Vol. 2. – P. 394-398.

4. Shrivastava, R.J. Land cover classification and economic assessment of citrus groves using remote sensing / R.J. Shrivastava, J.L. Gebelein / Journal of Photogrammetry and Remote Sensing. – 2007. – Vol. 61. – P. 341-353.

5. Verstraete, M.M. Designing optimal spectral indices for remote sensing applications / M.M. Verstraete, B. Pinty // IEEE Transactions on Geoscience and Remote Sensing. – 1996. – Vol. 34, № 5. – P. 1254-1265.

6. Using high spatial resolution nniltispectral data to classify corn and soybean crops / G.B. Senay [et al.] // Photogrammetric engineering and remote sensing. – 2000. – Vol. 66, No. 3. – P. 319-327.

7. Rubtsov, S.A. Aerospace equipment and technologies for precision farming / S.A. Rubtsov, I.N. Golovanev. A.N. Kashtanov. – M., 2008. – 330 p. [In russian]

8. Laneve, G. Continuous monitoring of forest res in mediterranean area using MSG / G. Laneve, M.M. Castronuovo, E.G. Cadau // IEEE Transactions on Geoscience and Remote Sensing. – 2006. – Vol. 44, No. 10. – P. 2761-2767.

9. Maselli, F. Evaluation of statistical methods to estimate forest volume in a Mediterranean region / F. Maselli, M. Chiesi // IEEE Transactions on Geoscience and Remote Sensing. – 2006. – Vol. 44, No. 8. – P. 2239-2250.

10. de Wasseige, C. Retrieval of tropical forest structure characteristics from bi-directional reflectance of SPOT images / C. deWasseige, P. Defourny // Remote Sensing of Environment. – 2002. – Vol. 83. – P. 362-375.

11. Roy, D.P. Remote sensing of re severity: assessing the performance of the Normalized Burn Ratio / D.P. Roy, L. Boschetti, S. Trigg // IEEE Geoscience and Remote Sensing Letters. – 2006. – Vol. 3, No. 1. – P. 112-116.

12. Ritchie, J.C. Remote sensing techniques to assess water quality / J.C. Ritchie, P.V. Zimba, J.H. Everitt // Photogrammetric Engineering and Remote Sensing. – 2003. – Vol. 69, No. 6. – P. 695-704.

13. Turner, M.G. Landscape ecology in theory and practice / M.G. Turner, R.H. Gardner, R.V. O'Neill. – Springer-Verlag, 2001. – 417 p.

14. Belyaev, B.I. Optical remote sensing / B.I. Belyaev, L.V. Katkovsky. – Minsk: BSU, 2006. – 455 p. [In russian]

15. Kumar, N. Do leaf surface characteristics affect agrobacterium infection in tea [Camellia Sinensis (L.) O Kuntze]? / N. Kumar, S. Pandey, A. Bhattacharya, P.S. Ahuja // J. Biosci. – 2004. – Vol. 29, No. 3. – P. 309–317.

16. Wu, Lanlan. Identification of weed/corn using BP network based on wavelet features and fractal dimension / Lanlan Wu, Youxian Wen, Xiaoyan Deng, Hui Peng // Scientific Research and Essay, November, 2009. – Vol.4 (11). – P. 1194-1200.

17. Qin, Z. Detection of rice sheath blight for in-season disease management using multispectral remote sensing / Zhihao Qin, Minghua Zhang // International Journal of Applied Earth Observation and Geoinformation, August, 2005. – Vol. 7, Issue 2, P. 115-128.

18. Aksoy, S. Automatic Mapping of Linear Woody Vegetation Features in Agricultural Landscapes Using Very High-Resolution Imagery / S. Aksoy, H.G. Akcay, T. Wassenaar // IEEE Transactions on Geoscience and Remote Sensing. – January 2010. – No. 48 (1, 2). – P. 511-522.

19. Torre, M., Agricultural field extraction on aerial images by region competition algorithm / M. Torre, P. Radeva // Int. Conf. on Pattern Recognition (ICPR'00), September 3-8, 2000, Barcelona, Spain. – Barcelona: 2000. – P. 137-139.

20. Inyutin, A.V., The algorithm of image segmentation by grayscale pseudoskeleton / A.V. Inyutin // Proceedings of the III International Conferences on Neural Networks and Arti cial Intelligence (ICNNAI'2003), November 12-14, Minsk, Belarus, 2003. – Minsk: Publishing center of BSU, 2003. – P. 263-265.

21. Soille, P. Morphological image analysis applied to crop field mapping / P. Soille // Image and Vision Computing. – 1973. – Vol. 18, No. 13. – P. 1025-1032.

22. Tzionas, P., Plant leaves classification based on morphological features and a fuzzy surface selection technique / P. Tzionas, S.E. Papadakis, D. Manolakis // 5th Int. Conf. on Technology and Automation (ICTA'05), 15-16 October 2005, Thessaloniki, Greece. – 2005. – P. 365-370.

23. Spectral discrimination and separability analysis of agricultural crops and soil attributes using aster imagery / A. Apan [et al.] // Proc. of 11th Australasian Remote Sensing and Photogrammetry Conference, 2-6 September, Brisbane, Queensland. – 2002. – P. 396-411.

24. Burks, T.F. Classification of weed species using color texture features and discriminant analysis / T.F. Burks, S.A. Shearer, F.A. Payne // Transactions of ASAE. – 2000. – Vol. 43 (2). – P. 441-448.

25. Detection and analysis of stochastic data and digital images / S.V. Ablameyko [et al] // Bulletin of the Foundation for Fundamental Research. –2003. – No. 4. – P. 101-106. [In russian]

26. Introduction to contour analysis; applications to image processing and signal / Ya.A. Furman [et al]. – M.: Fizmatlit, 2003. – 592 p. [In russian]

27. Kerfoot, I.B. Theoretical analysis of multispectral image

segmentation criteria / I.B. Kerfoot, Y. Bresler // IEEE Trans. Image Processing. – 1999. – Vol. 8, No. 6. – P. 768-820.

28. Coleman, G.B. Image segmentation by clustering / G.B. Coleman, H.C. Andrews // Proc IEEE. – 1979. – Vol. 67. – P. 773–785.

29. Zhang, Z. A survey on evaluation methods for image segmentation / Z. Zhang // Pattern Recognition. – 1996. – Vol. 29 (8). – P. 1335-1346.

30. Carpenter, G.A. A neural network method for efficient vegetation mapping / G.A. Carpenter, S. Gopal, C.E. Woodcock // Remote Sensing Environment. – 1999. – Vol. 70, No. 9. – P. 326-338.

31. Remote sensing of vegetation using modular neural networks / N. Kussul [et al.] // Proceedings of the III International Conferences on Neural Networks and Artificial Intelligence (ICNNAI'2003), November 12-14, Minsk, Belarus, 2003. – Minsk: Publishing center of BSU, 2003. – P. 232-234.

32. A neural network method for efficient vegetation mapping / C.C. Yang [et al.] // Recognition of Weeds with Image Processing and their use with Fuzzy Logic for Precision Farming. – Canadian Agricultural Engineering, 2000. – No. 42(4). – P. 195-200.

33. Tseng, Y.H., Automatic detecting rice fields by using multispectral satellite images, land-parcel data and domain knowledge / Y.H. Tseng, P.H. Hsu, Y.H. Chen // Proceedings of the 19th Asian Conference on Remote Sensing, Manila, Philippines, 16-20 November, 1998. – Minsk: 1998. – P. R–1–1~R–1–7.

34. Haas, T.C. Kriging and automated variogram modeling within a moving window / T.C. Haas // Atmospheric Environment. Part A. General Topics. –1990. – Vol. 24 (7). – P. 1759-1769.

35. Whelan, B.M. Spatial prediction for precision agriculture / B.M. Whelan, A.B. McBratney, R.A. Viscarra-Rossel // In Proceedings of the 3rd international conference on precision agriculture, Minneapolis, Minessota, June 23-26, 1996. – 1996. – P. 331-342.

36. Spatial prediction of topsoil salinity in the chelif valley, algeria, using local kriging with local variograms versus local kriging with whole-area variogram / C. Walter [et al.] // Australian Journal of Soil Research. – 2001. – Vol. 39. – P. 259-272.

37. Lucieer, A. Texture-based segmentation of high-resolution remotely sensed imagery for identification of fuzzy objects / Arko Lucieer, Peter Fisher, Alfred Stein // International Journal of Remote Sensing. – 2005. – No. 26(14). – P. 2917-2936.

38. Popescu, D. Carriage road pursuit based on statistical and fractal analysis of the texture / Dan Popescu, and Radu Dobrescu // International Journal of Education and Information Technologies. – 2008. – Vol. 2, Issue 1. – P. 62-70.

39. Emerson, Charles W. Multi-Scale Fractal Analysis of Image Texture and Pattern / Charles W. Emerson, Nina Siu-Ngan Lam, Dale A. Quattrochi // Photogrammetric Engineering & Remote Sensing. – January 1999. – Vol. 65, No. 1. – P. 51-61.

40. Starovoytov, V.V. Local geometric methods of digital image processing and analysis / V.V. Starovoytov. – Minsk: Institute of Technical Cybernetics of BAS. 1997. – 284 p. [In russian]

41. Haralick, R.M., Shanmugam K., Dinstein I. Textural Features for Image Classification // IEEE Transactions on Systems, Man and Cybernetics. – 1973. – No.6. – P. 610-621.

42. Feder, J. Fractals. New York: Plenum Press, 1988. – 283 p.

43. Potapov. A.A. Fractals in Radiophysics and Radiolocation / A.A. Potapov. – M.: Logos, 2002. – 664 p. [In russian]

44. Nigmatullin, R.R. Fractals, fractional operators and fractional kinetics in dielectric spectroscopy and wave processes / R.R. Nigmatullin, A.A. Potapov // Physics of wave processes and radio system. – 2007. – T. 10, No. 3. – P. 30-49. [In russian]

45. Ganchenko, V. Joint segmentation of Aerial Photographs with the Various Resolution / V. Ganchenko, A. Petrovsky, B. Sobkoviak // Proc. of the 5th Int Conf on Neural Networks and Artificial Intelligence ICNNAI 2008, May 27-30, 2008, Minsk, Belarus – Minsk, 2008. – P. 177-181.

46. Haykin, S. Neural networks: A Comprehensive Foundation, Second Edition. – Pearson Education, Inc, 2005. – 823 p.

47. Peter S. Pacheco, Parallel Programming with MPI, San Francisco, CA, Morgan Kaufmann, 1997. – 418 p.

48. M. Mitchell, J. Oldham and A. Samuel, “Advanced Linux Programming”, Indianapolis: New Riders Publishing, 2001. – 368 p.

49. The SKIF K-1000 Supercomputer 2.5 Tflops [Electronic document] – Access mode: http://skif.pereslavl.ru/psi-info/rcms/rcms-leaflets.eng/skif-k1000-leaflet-engl.pdf – 2004.

50. Joint belarussian-russian program “SKIF” [Electronic document] – Access mode: http://skif.bas-net.by/index_en.htm – 2004.